

The first basic study on natural convection in cylindrical annuli was carried out by Beckman, 1931 and extended by Kraussold, 1934. Further, a very comprehensive analysis has been made on the same geometry by Kuehn & Goldstein, 1978. They have conducted both numerical simulation using finite elements technique and experimental study using a Mach-Zehnder interferometer. Application of other type of finite differences method with ADI numerical solution has also been reported by Charrier-Mojtabi et al, 1979 who solved for laminar flow in horizontal concentric annuli using cylindrical polar coordinates.

Small eccentric annuli were studied in the work of Yao, 1980, using an expansion in terms of the double series of eccentricity and Rayleigh number for small values of Ra . The work of Cho et al, 1982 extended the knowledge on the natural convection heat transfer in horizontal cylindrical annuli. Therein, numerical analysis has been carried out using finite difference method in a bipolar coordinate system based on successive-over-relaxation iteration method.

Recent work of Kenjeres & Hanjalic, 1995, reports modeling and computational studies of natural convection in concentric and eccentric annuli by means of several variants of the algebraic stress model, based on the expression for turbulent heat flux $\overline{\theta u_i}$ obtained by truncation of the second-moment transport equation for this correlation. Various levels of closure were used including the low-Re number form of the k- ϵ model and a version in which differential transport equations are solved for the temperature variance $\overline{\theta^2}$ and its decay rate ϵ_θ .

Natural convection in cylindrical annular geometry filled with porous material has been studied by distinct numerical approaches, such as the finite-difference method reported by Caltagirone, 1976 and Burns & Tien, 1979. Finite element method is also found in the work of Charrier-Mojtabi et al, 1987 and the Galerkin spectral method in the work of Charrier-Mojtabi & Caltagirone, 1980, Rao et al, 1987 and Himasekhar & Bau, 1988. Charrier-Mojtabi et al, 1991, have shown that the Fourier-Chebyshev method gives better accuracy than does the full Fourier-Galerkin method for the description of two-dimensional multicellular flows.

Experimental studies using the Christiansen effect to visualize the thermal two-dimensional fields have been carried out by Cloupeau & Klarsfeld, 1973. In contrast with analytical studies, experiments have only unveiled unicellular flows. Additional experimental work of Caltagirone, 1976 and Charrier-Mojtabi et al, 1991 have shown the existence of various convective regimes.

Following this path, the work of Braga & de-Lemos, (2002a), presented results for laminar natural convection in a square cavity heated on the sides. Later, Braga & de-Lemos, (2002b) extended their results for considering laminar natural convection in a horizontal annular cavity. Turbulent regime in horizontal cylindrical annuli, both for concentric and eccentric cases, was also calculated (Braga & de-Lemos, (2002c)). Further, the study of natural convection in cavities completely filled with porous material was reported in the work of Braga & de-Lemos, (2002d). In that work the two geometries mentioned above, namely square and annular cavities, were considered. Further, the work of Braga & de-Lemos, (2002e) presented results for both laminar and turbulent flows in a square cavity heated from the left side and cooled from the opposing side for both clear and porous media. Results were compared with numerical data available in the literature. The turbulence model adopted was the standard k- ϵ with wall function.

Extending further the foregoing work on natural convection in clear and porous enclosures, this work presents results for both laminar and turbulent regime in a concentric horizontal cylindrical annulus completely filled with porous material. Results are compared with numerical data available in the literature.

One should mention, first of all, that studies on turbulent natural convection in porous media are not commonly available in the literature. With this limitation in mind, the main objective of this paper is to validate a numerical tool for simulating natural convection first in laminar regime and then in turbulent regime.

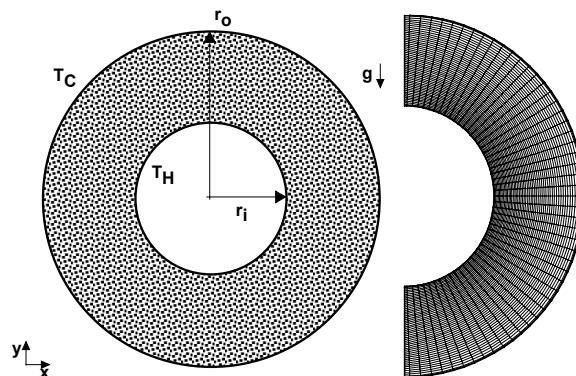


Figure 1. The geometry and the grid under consideration.

3. The Problem Considered

Figure 1 refers to a concentric annulus completely filled with porous material with outer and inner radii r_o and r_i , respectively, and $R=2$. The cavity, assumed to be of infinite depth along z -axis, is isothermally heated from the inner

cylinder and cooled at the outer surface. The non-slip condition is applied to the velocity field at all walls and the resulting flow is treated as steady.

4. Governing Equations

The equations used herein are derived in details in the work of Pedras & de-Lemos, 2001 and Rocamora & de-Lemos, 2000, and for that no specific derivation is here repeated. Basically, for porous media analysis, a macroscopic form of the governing equations is obtained by taking the volumetric average of the entire equation set. In that development, the porous medium is considered to be rigid and saturated by an incompressible fluid.

The macroscopic continuity equation is given by,

$$\nabla \cdot \bar{\mathbf{u}}_D = 0 \quad (1)$$

where the Dupuit-Forchheimer relationship, $\bar{\mathbf{u}}_D = \phi \langle \bar{\mathbf{u}} \rangle^i$, has been used and $\langle \bar{\mathbf{u}} \rangle^i$ identifies the intrinsic (liquid) average of the local velocity vector $\bar{\mathbf{u}}$.

This work extends the development in Pedras & de-Lemos, 2001, in order to include the buoyancy term in the governing equations. Accordingly, the Boussinesq hypothesis can be written as, $\rho = \rho_{ref} [1 - \beta(\bar{T} - T_{ref})]$. Substituting this term in the momentum equation, the buoyancy term reduces to,

$$\rho_{ref} g \beta (\bar{T} - T_{ref}) \quad (2)$$

Applying the volumetric average one has,

$$\langle \rho_{ref} g \beta (\bar{T} - T_{ref}) \rangle^v = \frac{\Delta V_f}{\Delta V} \frac{1}{\Delta V_f} \int \rho_{ref} g \beta (\bar{T} - T_{ref}) dV \quad (3)$$

Therefore, the buoyancy term becomes,

$$\rho_{ref} \beta_\phi g \phi \langle \bar{T} \rangle^i - T_{ref} \quad (4)$$

With the **Macroscopic Buoyancy Term** given by 4, the macroscopic time-mean Navier-Stokes (NS) equation for an incompressible fluid with constant properties is given as,

$$\rho \left[\frac{\partial \bar{\mathbf{u}}_D}{\partial t} + \nabla \cdot \left(\frac{\bar{\mathbf{u}}_D \bar{\mathbf{u}}_D}{\phi} \right) \right] = -\nabla(\phi \langle \bar{p} \rangle^i) + \mu \nabla^2 \bar{\mathbf{u}}_D + \nabla \cdot \left(-\rho \phi \langle \bar{\mathbf{u}} \bar{\mathbf{u}} \rangle^i \right) + \rho_{ref} \beta_\phi g \phi \langle \bar{T} \rangle^i - T_{ref} \left[\frac{\mu \phi}{K} \bar{\mathbf{u}}_D + \frac{c_F \phi \rho \langle \bar{\mathbf{u}}_D \rangle \bar{\mathbf{u}}_D}{\sqrt{K}} \right] \quad (5)$$

Further, when treating turbulence with statistical tools, the correlation $-\rho \overline{\mathbf{u}} \bar{\mathbf{u}}$ appears after application of the time-average operator to the local instantaneous NS equation. Applying further the volume-average procedure to this correlation results in the term $-\rho \phi \langle \bar{\mathbf{u}} \bar{\mathbf{u}} \rangle^i$, as can be seen in the equation 5 above. This term is here recalled as the **Macroscopic Reynolds Stress Tensor** (MRST). A model for the MRST in analogy with the Boussinesq concept for clear fluid can be written as:

$$-\rho \phi \langle \bar{\mathbf{u}} \bar{\mathbf{u}} \rangle^i = \mu_{t_\phi} 2 \langle \bar{\mathbf{D}} \rangle^v - \frac{2}{3} \phi \rho \langle k \rangle^i \mathbf{I} \quad (6)$$

where

$$\langle \bar{\mathbf{D}} \rangle^v = \frac{1}{2} \left[\nabla \langle \phi \bar{\mathbf{u}} \rangle^i + \left[\nabla \langle \phi \bar{\mathbf{u}} \rangle^i \right]^T \right] \quad (7)$$

is the macroscopic deformation tensor, $\langle k \rangle^i$ is the intrinsic average for k and μ_{t_ϕ} is the macroscopic turbulent viscosity. The macroscopic turbulent viscosity, μ_{t_ϕ} , is modeled similarly to the case of clear fluid flow and a proposal for it was presented in Pedras & de-Lemos, 2001 as,

$$\mu_{t_\phi} = \rho c_\mu \frac{\langle k \rangle^i}{\langle \varepsilon \rangle^i} \quad (8)$$

In a similar way, applying both time and volumetric average to the microscopic energy equation, for either the fluid or the porous matrix, two equations arise. Assuming further the **Local Thermal Equilibrium Hypothesis**, which considers $\langle \overline{T}_f \rangle^i = \langle \overline{T}_s \rangle^i = \langle \overline{T} \rangle^i$, and adding up these two equations, one has,

$$\left\{ (\rho c_p)_f \phi + (\rho c_p)_s (1-\phi) \right\} \frac{\partial \langle \overline{T} \rangle^i}{\partial t} + (\rho c_p)_f \nabla \cdot (\overline{\mathbf{u}}_D \langle \overline{T} \rangle^i) = \nabla \cdot \left\{ [k_f \phi + k_s (1-\phi)] \nabla \langle \overline{T} \rangle^i \right\} + \nabla \cdot \left[\underbrace{\frac{1}{\Delta V} \int_{A_i} \mathbf{n} (k_f \overline{T}_f - k_s \overline{T}_s) dS}_I - (\rho c_p)_f \nabla \cdot \left[\phi \left(\underbrace{\langle \mathbf{u}' \rangle^i \langle T_f' \rangle^i}_{II} + \underbrace{\langle \overline{\mathbf{u}}^i \overline{T}_f \rangle^i}_{III} + \underbrace{\langle \mathbf{u}'^i T_f' \rangle^i}_{IV} \right) \right] \right] \quad (9)$$

where to each underscored term on the right hand side of Eq. (9), the following significance can be attributed: I-**Tortuosity** - based on the stagnant heat path inside the porous medium, II-**Turbulent Heat Flux** - due to the macroscopic time fluctuations of the velocity and the temperature, III-**Thermal Dispersion** - associated to the spatial deviations of the time averaged microscopic velocity and temperature. Note that this term is also present in laminar flows in porous media., IV-**Turbulent Thermal Dispersion** - due to both time fluctuations and spatial deviations of the microscopic velocity and temperature.

A modeled form of equation (9) has been given in detail in the work of de-Lemos & Rocamora, 2002, and Rocamora & de-Lemos, 2002, as,

$$\left\{ (\rho c_p)_f \phi + (\rho c_p)_s (1-\phi) \right\} \frac{\partial \langle \overline{T} \rangle^i}{\partial t} + (\rho c_p)_f \nabla \cdot (\mathbf{u}_D \langle \overline{T} \rangle^i) = \nabla \cdot \left\{ \mathbf{K}_{eff} \cdot \nabla \langle \overline{T} \rangle^i \right\} \quad (10)$$

where, \mathbf{K}_{eff} , given by:

$$\mathbf{K}_{eff} = \left[\phi k_f + (1-\phi) k_s \right] \mathbf{I} + \mathbf{K}_{tor} + \mathbf{K}_t + \mathbf{K}_{disp} + \mathbf{K}_{disp,t} \quad (11)$$

is the effective conductivity tensor. In order to be able to apply Eq. (10), it is necessary to determine the conductivity tensors in Eq. (11), *i.e.*, \mathbf{K}_{tor} , \mathbf{K}_t , \mathbf{K}_{disp} and $\mathbf{K}_{disp,t}$. Following Kuwahara & Nakayama (1998), this can be accomplished for the tortuosity and thermal dispersion conductivity tensors, \mathbf{K}_{tor} and \mathbf{K}_{disp} , by making use of a unit cell subjected to periodic boundary conditions for the flow and a linear temperature gradient imposed over the domain. The conductivity tensors are then obtained directly from the microscopic results for the unit cell (see Kuwahara & Nakayama (1998) for details on the expressions here used).

The turbulent heat flux and turbulent thermal dispersion terms, \mathbf{K}_t and $\mathbf{K}_{disp,t}$, which cannot be determined from such a microscopic calculation, are modeled here through the Eddy diffusivity concept, similarly to Nakayama & Kuwahara (1999). It should be noticed that these terms arise only if the flow is turbulent, whereas the tortuosity and the thermal dispersion terms exist for both laminar and turbulent flow regimes.

Starting out from the time averaged energy equation coupled with the microscopic modeling for the ‘turbulent thermal stress tensor’ through the Eddy diffusivity concept, one can write, after volume averaging,

$$-(\rho c_p)_f \langle \overline{\mathbf{u}' T_f'} \rangle^i = (\rho c_p)_f \frac{\nu_{t_\phi}}{\sigma_T} \nabla \langle \overline{T} \rangle^i \quad (12)$$

where the symbol ν_{t_ϕ} expresses the macroscopic Eddy viscosity, $\mu_{t_\phi} = \rho_f \nu_{t_\phi}$, given by (8) and σ_T is a constant. According to equation (12), the macroscopic heat flux due to turbulence is taken as the sum of the turbulent heat flux and the turbulent thermal dispersion found by Rocamora & de-Lemos, 2000. In view of the arguments given above, the turbulent heat flux and turbulent thermal dispersion components of the conductivity tensor, \mathbf{K}_t and $\mathbf{K}_{disp,t}$, respectively, are expressed as:

$$\mathbf{K}_t + \mathbf{K}_{disp,t} = \phi (\rho c_p)_f \frac{\nu_{t_\phi}}{\sigma_T} \mathbf{I} \quad (13)$$

In the equation set shown above, when the variable $\phi=1$, the domain is considered as a clear medium. For any other value of ϕ , the domain is treated as a porous medium.

5. Numerical Method and Solution Procedure

The numerical method employed for discretizing the governing equations is the control-volume approach with a collocated grid. A hybrid scheme, Upwind Differencing Scheme (UDS) and Central Differencing Scheme (CDS), is used for interpolating the convection fluxes.

The well-established SIMPLE algorithm (Patankar & Spalding, 1972) is followed for handling the pressure-velocity coupling. Individual algebraic equation sets were solved by the SIP procedure of Stone, 1968.

6. Turbulence Transport Equations

Transport equations for $\langle k \rangle^i = \overline{\langle \mathbf{u}' \cdot \mathbf{u}' \rangle}^i / 2$ and $\langle \varepsilon \rangle^i = \mu \overline{\langle \nabla \mathbf{u}' : (\nabla \mathbf{u}')^T \rangle}^i / \rho$ in their so-called High Reynolds number form are proposed in Pedras & de-Lemos, 2001 as:

$$\rho \left[\frac{\partial}{\partial t} (\phi \langle k \rangle^i) + \nabla \cdot (\bar{\mathbf{u}}_D \langle k \rangle^i) \right] = \nabla \cdot \left[\left(\mu + \frac{\mu_{t\phi}}{\sigma_k} \right) \nabla (\phi \langle k \rangle^i) \right] + P^i + G^i + G_k^i - \rho \phi \langle \varepsilon \rangle^i \quad (14)$$

$$\rho \left[\frac{\partial}{\partial t} (\phi \langle \varepsilon \rangle^i) + \nabla \cdot (\bar{\mathbf{u}}_D \langle \varepsilon \rangle^i) \right] = \nabla \cdot \left[\left(\mu + \frac{\mu_{t\phi}}{\sigma_\varepsilon} \right) \nabla (\phi \langle \varepsilon \rangle^i) \right] + \frac{\langle \varepsilon \rangle^i}{\langle k \rangle^i} [c_1 P^i + c_2 G^i + c_1 c_3 G_k^i - c_2 \rho \phi \langle \varepsilon \rangle^i] \quad (15)$$

where c_1 , c_2 , c_3 and c_k are constants, $P^i = (-\rho \overline{\langle \mathbf{u}' \cdot \mathbf{u}' \rangle}^i : \nabla \bar{\mathbf{u}}_D)$ is the production rate of $\langle k \rangle^i$ due to gradients of $\bar{\mathbf{u}}_D$ and $G^i = c_k \rho \frac{\phi \langle k \rangle^i |\bar{\mathbf{u}}_D|}{\sqrt{K}}$ is the generation rate of the intrinsic average of k due to the action of the porous matrix.

This work extends the development therein in order to include the buoyancy production rate term in the turbulence model equations. For clear flows the buoyancy contribution to the k equation reads,

$$G_k = -\frac{v_t}{\sigma_t} g \beta \frac{\partial \bar{T}}{\partial y} \quad (16)$$

Applying the volumetric average one has,

$$\left\langle -\frac{v_t}{\sigma_t} g \beta \frac{\partial \bar{T}}{\partial y} \right\rangle^v = \frac{\Delta V_f}{\Delta V} \frac{1}{\Delta V_f} \int -\frac{v_t}{\sigma_t} g \beta \frac{\partial \bar{T}}{\partial y} dV \quad (17)$$

The final form of the buoyancy production rate term is then,

$$G_k^i = -\phi \frac{v_{t\phi}}{\sigma_t} g \beta_\phi \frac{\partial \langle \bar{T} \rangle^i}{\partial y} \quad (18)$$

7. Results and Discussion

7.1. Laminar Flow Solution

Many workers have focused their attention on the bifurcation and stability of the numerical solution. This work has not this intention and its objective is to validate the numerical tool comparing the present results with others numerical and experimental works. Calculations were then performed for half domain using a 50x50 grid on the geometry shown in Fig. 1.

According Caltagirone, 1976, there are three convection regimes. The first one is where the Rayleigh number $Ra^* = g \beta (\rho c)_f \Delta T K r_i / k_{eff} \nu$ is less or equal than 8, convective phenomena are very little developed and heat transfer occurs only by conduction. This regime will be called *pseudo-conduction*. The second one is in the interval $8 < Ra^* < 65$ and onvective currents are found to be steady. The fluid warms up on contact with the inner cylinder and fall along the outer surface. The last regime is for $Ra^* > 65$ where a new type of evolution appears. Perturbations occur in the upper part of the annular layer and are shown by fluctuations in temperature. Experimental observations suggest that, for high Rayleigh numbers, the fluid flow domain can be divided into five regions, (Himasekhar & Bau, 1988) as shown in Tab 1.

Table 1 – Domain important regions

Region	Description
<i>Inner boundary layer</i>	A thin thermal layer near the inner cylinder in which gradients in the angular direction are negligible compared to those in the radial direction.
<i>Outer boundary layer</i>	A thin thermal layer near the outer cylinder in which gradients in the angular direction are negligible compared to those in the radial direction.
<i>Plume</i>	Exits along the vertical line of symmetry above the inner cylinder and joins the inner and outer thermal layers.
<i>Stagnant region</i>	A region, located beneath the inner cylinder, in which the buoyancy forces inhibits fluid motion and the heat transfer is purely by conduction.
<i>Core region</i>	The one bounded by the other four regions.

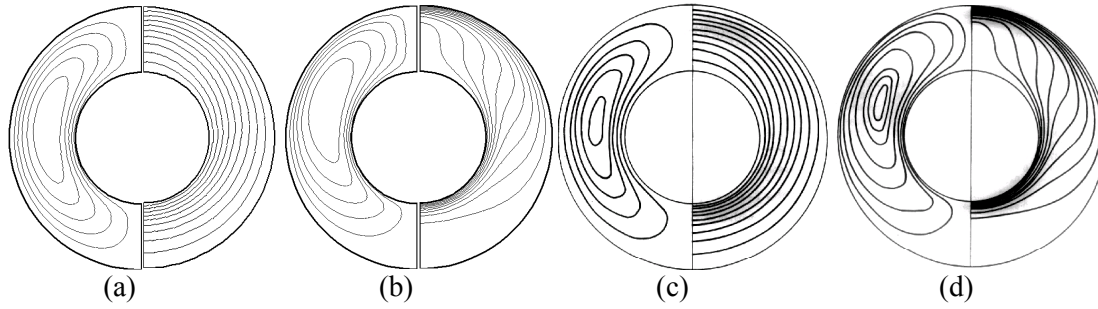


Figure 2 – Laminar solution. Isotherms and Streamlines for a $Ra^* = 2.5 \times 10$, $Ra^* = 2.0 \times 10^2$ and $R=2$; (a), (b): Present results; (c), (d): Caltagirone, 1976.

Figure 2 shows calculated laminar isotherms and streamlines for a concentric annular cavity, heated from the inner cylinder and cooled at the outer surface, completely filled with porous material for $Ra^* = 2.5 \times 10$, $Ra^* = 2 \times 10^2$ and $R=2$. The figures show a good agreement of the present simulations with the work of Caltagirone, 1976, reproducing the basic features of the flow.

Table 2 shows, for some Rayleigh numbers, the average Nusselt number \overline{Nu} on the heated inner cylinder. It is seen from this table that the agreement between the present and previous results seems to be reasonable. The heat transfer coefficient is seen to increase with Ra^* distorting the isotherms as convection becomes dominant although the streamlines do not presents such intense variations, see Fig. 2.

Table 2. Average Nusselt number \overline{Nu} for Rayleigh numbers ranging from 25 to 500.

	Ra^*				
	25	100	150	200	500
Caltagirone, 1976	1.0993	1.8286	-	2.6256	4.1983
Charrier-Mojtabi, 1997	-	1.8670	2.3090	-	-
Present results – laminar flow solution	1.1079	1.8602	2.2961	2.6662	4.2306

7.2. Turbulent Flow Solution

Calculations for turbulent flow were performed for half domain using a 50×50 grid on the geometry shown in Fig. 1. Figure 3 shows the streamlines and isotherms of a horizontal concentric annuli cavity completely filled with porous material heated from the inner cylinder and cooled from the outer for $Ra^* = 2.5 \times 10$ and 2×10^2 and for $R=2$.

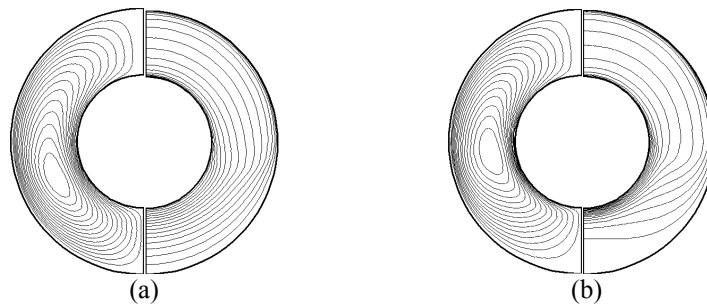


Figure 3. Turbulent solution. Isotherms and Streamlines for $R=2$: a) $Ra^* = 2.5 \times 10$, b) $Ra^* = 2.0 \times 10^2$

When the standard k- ϵ model is used for low Ra^* values, the results do not represent an exact laminar solution (with zero turbulent viscosity) since the transport equation set (1)-(5)-(10)-(14)-(15) is valid for high Re flows and is solved with the wall function approach for handling the wall proximity. Therefore, below a certain critical Rayleigh number, the standard k- ϵ model gives a turbulent viscosity, which is close to zero everywhere and the solution can be interpreted as an approximation of the laminar flow regime. But, above this critical value, the turbulent viscosity suddenly increases and a turbulent solution is obtained.

Comparing the laminar and the turbulent solution for the same Ra^* numbers (Figs 2 and 3), one can note that for the smaller Ra^* , Fig. 3(a), both cases (laminar and turbulent flow solutions) does show remarkable differences and the flow pattern remains almost the same with the center of the streamlines a little dislocated downward for the turbulent case. For the higher Ra^* number, the isotherms presented in Fig. 3(b) in the region located beneath the inner cylinder show a similar behavior when compared with those from the laminar case, in which the buoyancy forces inhibits fluid motion and the heat transfer is purely by conduction. However, at the upper part of the annulus, Fig. 3(b) does not show a

plume above the inner heated cylinder as appears in the laminar case of Fig. 2(b). This is probably associated with the high levels of turbulent kinetic energy in such region, inducing a higher overall heat flux from the inner surface towards the outer cylinder. Figure 4 shows corresponding isolines of turbulent kinetic energy for $Ra^*=2.0 \times 10^2$ and $R=2$. The figure clearly shows that in the upper part of the annular region the turbulent kinetic energy presents its highest levels.



Figure 4. Isolines of turbulent kinetic energy for $Ra^*=2.0 \times 10^2$ and $R=2$.

Corresponding temperature profiles across the gap are presented in Figure 5. The figure shows the behavior of the macroscopic temperature at the symmetry line above the inner cylinder for $Ra^*=2.0 \times 10^2$ and $R=2$, using laminar and turbulent flow solutions. As indicated by the figure, the turbulent solution shows a more gradual temperature distribution across the entire gap when compared with the one for the laminar case. The steeper temperature gradient at the inner wall indicates that more heat is transferred through the gap. This enhancement of heat transfer is coherent with the large values for k within that same region.

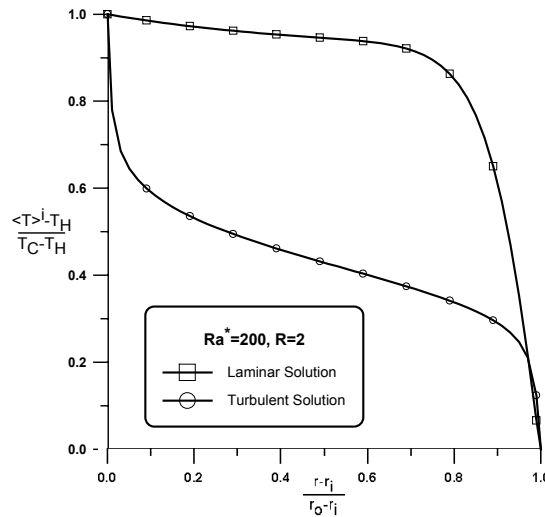


Figure 5. Macroscopic temperature behavior at the symmetry line above the inner cylinder for $Ra^*=2.0 \times 10^2$ and $R=2$, for laminar and turbulent regime.

Table 3. Average Nusselt numbers \overline{Nu} for Rayleigh numbers ranging from 10 to 500.

	Ra^*				
	10	25	100	200	500
Present results – laminar flow solution	1.108	1.860	2.296	2.666	4.231
Present results – turbulent flow solution	3.735	4.689	6.852	7.984	9.450

Table 3 finally shows, for selected Rayleigh numbers, the average Nusselt number \overline{Nu} based on the heated inner cylinder. In comparison, the turbulent average Nusselt numbers are significantly greater than the ones obtained with a laminar model. A possible explanation for it is that the thin thermal boundary layer above the inner cylinder entails a steeper temperature gradient when turbulence is considered, increasing then the value of the average Nusselt number based on the inner cylinder. These results seem to be in agreement with all simulations shown so far.

8. Conclusions

This paper presented computations for simulation of laminar and turbulent natural convection in horizontal concentric annuli heated on the inner cylinder and cooled at the outer surface. The laminar results yielded generally satisfactory agreement with the numerical data available in the literature. For all case considered, there are a stagnant region below the inner cylinder. For turbulent cases, the isotherms above the inner heated cylinder for higher Ra^* numbers has a gradual temperature distribution when compared with those from the laminar ones, probably due to the high levels of turbulent kinetic energy in such region, inducing a larger heat flux from the inner wall. Finally, as expected, the overall turbulent Nusselt numbers are higher than those from the laminar cases.

9. Acknowledgments

The authors are thankful to CNPq, Brazil, for their financial support during the course of this research.

10. References

- Beckman, W., 1931, DIE WARMEUBERTRAGUNG IN ZYLINDRISCHEN GASSCHICHTEN BEI NATURLICHER KONVEKTION, *Forsch. Geb. Ing. Wes.*, Vol 2, pp. 165-178.
- Bérnard, H., 1901, LES TOURBILLONS CELLULAIRES DANS UNE NAPPE LIQUIDE TRANSPORTANT DE LA CHALEUR PAR CONVECTION EM RÉGIME PERMANENT, *Ann. Chim. Phys.*, vol 23, pp. 62-144.
- Braga, E.J., de-Lemos, M.J.S., 2002a, FREE CONVECTION IN SQUARE AND RECTANGULAR CAVITIES HEATED FROM BELOW OR ON THE LEFT, *Proceedings of CONEM2002, 3rd Congresso Nacional de Engenharia Mecânica*, João Pessoa, PB, Brazil, August 12-16.
- Braga, E.J., de-Lemos, M.J.S., 2002b, LAMINAR NATURAL CONVECTION IN CONCENTRIC AND ECCENTRIC ANNULI, *Proceedings of ENCIT2002, 9th Brazilian Congress of Thermal Engineering and Sciences* (accepted for presentation), Caxambu, MG, Brazil, October 13-17.
- Braga, E.J., de-Lemos, M.J.S., 2002c, NATURAL CONVECTION IN TURBULENT REGIME IN CONCENTRIC AND ECCENTRIC HORIZONTAL ANNULAR REGIONS, **Paper AIAA-2002-3316**, *Proc. of 8th AIAA/ASME, Joint Thermophysics and Heat Transfer Conference*, St Louis, Missouri, U.S.A, June 23-27.
- Braga, E.J., de-Lemos, M.J.S., 2002d, NATURAL CONVECTION IN CAVITIES COMPLETELY FILLED WITH POROUS MATERIAL, *Proceedings of APM2002, 1st International Conference on Applications of Porous Media*, **Paper APM-164**, vol. 1, pp. 551-560, Jerba, Tunísia, June 2-8.
- Braga, E.J., de-Lemos, M.J.S., 2002e, Turbulent Natural Convection in Enclosures With Clear Fluid and Completely Filled With Porous Material, **Paper IMECE2002-34403**, *2002 ASME International Mechanical Engineering Congress* (accepted for presentation), New Orleans, LA, USA, November 17-22, 2002.
- Burns, P.J., Tien, C.L., 1979, NATURAL CONVECTION IN POROUS MEDIUM BOUNDED BY CONCENTRIC SPHERES AND HORIZONTAL CYLINDERS, *Int. J. Heat Mass Transfer*, Vol 22, pp. 929-939.
- Caltagirone, J.P., 1976, THERMOCONVECTIVE INSTABILITIES IN A POROUS MEDIUM BOUNDED BY TWO CONCENTRIC HORIZONTAL CYLINDERS, *J. Fluid Mech*, Vol 76, part 2, pp. 337-362.
- Charrier-Mojtabi, M.C., 1997, NUMERICAL SIMULATION OF TWO –AND –THREEDIMENSIONAL FREE CONVECTION FLOWS IN A HORIZONTAL POROUS ANNULUS USING A PRESSURE AND TEMPERATURA FORMULATION, *Int. J. Heat Mass Transfer*, Vol 40, No 7, pp. 1521-1533.
- Charrier-Mojtabi, M.C., Caltagirone, J.P., 1980, NUMERICAL SIMULATION OF NATURAL CONVECTION IN AN ANNULAR POROS LAYER BY SPECTRAL METHOD, *Proc. 1st Int. Conf. Of Numerical Methods for Non-Linear Problems*, Swannsea, pp. 821-828.
- Charrier-Mojtabi, M.C., Mojtabi, A. and Caltagirone J.P., 1979, NUMERICAL SOLUTION OF FLOW DUE TO NATURAL CONVECTION IN HORIZONTAL CYLINDRICAL ANNULUS, *J. Heat Transfer*, Vol 101, pp. 171-173.
- Charrier-Mojtabi, M.C., Mojtabi, A., Azaiez, M., Labrosse, G., 1991, NUMERICAL AND EXPERIMENTAL STUDY OF MULTICELLULAR FREE CONVECTION FLOWS IN AN ANNULAR POROUS LAYER, *Int. J. Heat Mass Transfer*, Vol 34, pp. 3061-3074.
- Cho, C.H., 1982, NUMERICAL SIMULATION OF NATURAL CONVECTION IN CONCENTRIC AND ECCENTRIC HORIZONTAL CYLINDRICAL ANNULI, *J. Heat Transfer*, Vol 104, pp. 624-630.

- Cloupeau, M., Klarsfeld, S., 1973, VISUALIZATION OF THERMAL FIELDS IN SATURATED POROUS MEDIA BY CHRISTIANSEN EFFECT, *Applied Optics*, Vol 12, pp. 198-204.
- de-Lemos, M.J.S., Rocamora Jr, F.D., 2002, Turbulent Transport Modeling for Heated Flow in Rigid Porous Media, 12th. Intern. Heat Transfer Conference (*accepted for presentation*), Grenoble, France, August 18-23.
- Himasekhar, K., Bau, H.H., 1988, TWO DIMENSIONAL BIFURCATION PHENOMENA IN THERMAL CONVECTION IN HORIZONTAL CONCENTRIC ANNULI CONTAINING SATURATED POROUS MEDIA, *J. Fluid Mech*, Vol 187, pp. 267-300.
- Kenjeres, S., Hanjalic, K., 1995, PREDICTION OF TURBULENT THERMAL CONVECTION IN CONCENTRIC AND ECCENTRIC HORIZONTAL ANNULI, *Int. J. Heat and Fluid Flow*, Vol 16, pp. 429-439.
- Nakayama, A., Kuwahara, F., 1999, A Macroscopic Turbulence Model for Flow in a Porous Medium *Journal of Fluids Eng.*, **121**, 427-433.
- Kuwahara, F., Nakayama, A., Numerical modeling of non-Darcy convective flow in a porous medium, *Proc. 11th International Heat Transfer Conf.*, Kyongju, Korea, vol. 4, pp. 411-416, 1998.
- Kraussold, H., 1934, WARMEABGADE VON ZYLINDRISCHEN FLUSSIGKEITSSCHICHTEN BEI NATURLICHER KONVEKTION, *Forsch. Geb. IngWes.*, Vol 5, pp. 186-191.
- Kuehn, T.H., Goldstein, R.J., 1978, AN EXPERIMENTAL STUDY OF NATURAL CONVECTION HEAT TRANSFER IN CONCENTRIC AND ECCENTRIC HORIZONTAL CYLINDRICAL ANNULI, *J. Heat Transfer*, Vol 100, pp. 635-640.
- Mojtabi, A., Quazar, D., Charrier-Mojtabi, M.C., 1987, NA EFFICIENT FINITE ELEMENT CODE FOR 2D STEADY STATE IN A POROUS ANNULUS, *Proc. Int. Conf. Numerical Methods for Thermal Problems*, Montreal, Vol 5, pp. 644-654.
- Patankar, S.V., Spalding, D.B., 1972, A CALCULATION PROCEDURE FOR HEAT, MASS AND MOMENTUM TRANSFER IN THREE DIMENSIONAL PARABOLIC FLOEWS, *Int. J. Heat Mass Transfer*, Vol 15, pp. 1787.
- Pedras, M.H.J., de Lemos, M.J.S., 2001, MACROSCOPIC TURBULENCE MODELING FOR INCOMPRESSIBLE FLOW THROUGH UNDEFORMABLE POROUS MEDIA, *Int. J. Heat Mass Transfer*, Vol 44(6), pp. 1081-1093.
- Rao, Y. F., Fukuda, K., Hasegawa, S., 1987, STEADY AND TRANSIENT ANALYSIS OF NATURAL CONVECTION IN A HORIZONTAL POROUS ANNULUS WITH GALERKIN METHOD, *J. Heat Transfer*, Vol 109, pp. 919-927.
- Rayleigh, Lord (J. W. Strutt), 1926, ON CONVECTION CURRENTS IN A HORIZONTAL LAYER OF FLUID WHEN THE HIGHER TEMPERATURE IS ON THE UNDERSIDE, *Phil. Mag.*, ser. 6, Vol 32, pp.833-844.
- Rocamora Jr, F.D., de-Lemos, M.J.S., 2000, ANALYSIS OF CONVECTIVE HEAT TRANSFER FOR TURBULENT FLOW IN SATURATED POROUS MEDIA, *Int. Comm. Heat Mass Transfer*, Vol 27(6), pp. 825-834.
- Rocamora Jr, F.D., de-Lemos, M.J.S., 2002, NUMERICAL DETERMINATION OF THE THERMAL DISPERSION TENSOR IN AN INFINITE POROUS MEDIUM, *Numerical Heat Transfer* (submitted).
- Stone, H.L., 1968, ITERATIVE SOLUTION OF IMPLICIT APPROXIMATIONS OF MULTI-DIMENSIONAL PARTIAL DIFFERENTIAL EQUATIONS, *SIAM J. Num. Anal.*, Vol 5, pp. 530-558.
- Yao, L.S., 1980, ANALYSIS OF HEAT TRANSFER IN SLIGHTLY ECCENTRIC ANNULI, *J. Heat Transfer*, Vol 102, pp. 270-284.